



CrossMark  
 click for updates

Cite this: *RSC Adv.*, 2015, 5, 94599

## Fulleropyrrolidines derived from dioxo- and trioxaalkyl-tethered diglycines†

Tatjana Kop,<sup>a</sup> Mira Bjelaković,<sup>a</sup> Jelena Đorđević,<sup>b</sup> Andrijana Žekić<sup>c</sup> and Dragana Milić<sup>\*b</sup>

Two different  $\alpha,\omega$ -diglycines linked by linear polyoxaalkyl chains in the presence of formaldehyde underwent Prato reaction to the fullerene C<sub>60</sub>. The shorter linker templated formation of only *cis*-bisadducts, while the longer one afforded a mixture of four bisadducts (all *cis* and the *equatorial*) and difullerene dumbbell compound. Their structures were confirmed by the extensive analysis of the spectral data and molecular symmetry, as well. All compounds expressed an ability to arrange into hierarchically ordered supramolecular aggregates, the form of which depended both on the addition pattern and the spacer structure. The attenuated electron-accepting affinity, examined by cyclic voltammetry was in agreement with diminished delocalization of the  $\pi$ -electronic system. In addition, all compounds exerted a notable radical scavenging activity.

Received 27th August 2015  
 Accepted 29th October 2015

DOI: 10.1039/c5ra17392b

[www.rsc.org/advances](http://www.rsc.org/advances)

### 1 Introduction

Fullerene C<sub>60</sub> and its derivatives have been widely studied and employed in materials<sup>1</sup> and medicinal chemistry.<sup>2</sup> The functionalization of highly insoluble carbon sphere with remarkably useful properties provides hybrids with an optimal ratio of the target characteristics (such as antioxidant, radio protective, optical limiting activity, or ligand–host interactions) and the physical properties responsible for the suitable environmental adjustment (solubility and aggregation). Common cycloaddition reactions, known as Bingel cyclopropanation,<sup>3</sup> Diels–Alder cycloaddition<sup>4</sup> or Prato reaction,<sup>5</sup> covalently transform C<sub>60</sub> affording mono- or multiple adducts. The usability of polyadducts can be even better in comparison to the corresponding monoadducts,<sup>6</sup> but the application is often limited by formation of large number of regioisomers.<sup>7</sup> Multiplication of the addends on the fullerene core mostly contributes to the solubility and assembling capability due to enlarged number of possible intermolecular interactions. At the same time, a reduced delocalization of the molecular orbitals increases the HOMO–LUMO energy gap, such provoking a negative shift of reduction potentials in comparison to nonfunctionalized C<sub>60</sub>,<sup>8</sup> with exception of

addends possessing electron withdrawing groups proximal to the fullerene cage.<sup>9,6a–c</sup> Common bisaddition reactions usually provide low selectivity, implying demanding purification process although in some cases mixtures of bisadducts were subjected to a further examination without separation of the individual products.<sup>10</sup> Examples of cycloaddition reactions which resulted in complete separation and characterization of all synthesized bisadducts<sup>11</sup> demonstrated that *trans*-1 and *cis*-1 isomers are the least favoured in all three types of cycloaddition reactions. The *trans*-3 and *equatorial* adducts are the major products in Diels–Alder and Bingel reactions, while the amount of the *cis* isomers is almost negligible. The contribution of the *cis*-adducts in Prato bisaddition is much higher, making the *cis*-2 adduct one of the major products. Some of the first attempts to improve the selectivity of a bisaddition reaction included initial Diels–Alder monoadduct as a directing group in successive Bingel biscyclopropanation. After retro-Diels–Alder cycloaddition, improved amount of *cis*-methanofullerenes was achieved, but reaction was still insufficiently selective.<sup>12</sup> The first significant improvement in bisaddition selectivity was made when templated substrate wearing two different reacting groups at the opposite sides of aromatic spacing unit underwent Bingel reaction followed by Diels–Alder cycloaddition, selectively affording *equatorially* tethered bisadduct in 50% yield.<sup>13</sup> Since then, many of bis-malonates efficiently templated biscyclopropanation, yielding one major regioisomer of bis(methano)fullerenes tethered with *o*-, *m*- or *p*-xylenes,<sup>14</sup> Tröger bases,<sup>15</sup> phorphirin<sup>16</sup> or crown ethers.<sup>17</sup> Also, aromatic dialdehydes were used to template the regioselective formation of bis(pyrrolidino)fullerenes in the one-pot reaction,<sup>18</sup> or *via* isolated monoadduct and subsequent intramolecular addition.<sup>19</sup> However, the utilization of dialdehydes lead to the increment in the number of products due to

<sup>a</sup>Center for Chemistry, ICTM University of Belgrade, Njegoševa 12, 11000 Belgrade, Serbia

<sup>b</sup>Faculty of Chemistry, University of Belgrade, Studentski trg 12-16, 11158 Belgrade, Serbia. E-mail: dmilic@chem.bg.ac.rs

<sup>c</sup>Faculty of Physics, University of Belgrade, Studentski trg 12-16, 11158 Belgrade, Serbia

† Electronic supplementary information (ESI) available: Experimental section, tabular representation of the UV and the NMR data, the NMR and HRMS spectra, additional SEM images, the CV curves of compounds 3–14, and their HPTLC densitograms. See DOI: 10.1039/c5ra17392b

stereocenter formation in pyrrolidinic rings. To avoid it, we have recently examined a different approach to one-pot Prato bisaddition using formaldehyde and simple, alkyl-bridged diglycines as a model system.<sup>20</sup> With precursors containing medium to long alkyl-tethers, the number of isolated bis(pyrolidino)fullerenes was rapidly reduced from eight possible to only two or three, having in majority of reactions clearly defined the major isomer over the other bisadducts. The length of the tether and the addition pattern influenced both spectroscopic properties and the shape of the hierarchically organized supramolecular structures. In addition, a significant *in vitro* antioxidant activity of such obtained bisadducts was confirmed. All of the results encouraged us to expand this reaction to other linkers and to establish their effect on regioselectivity and the products properties. Having in mind that alkyl chains enriched with two or more ether subunits have been already proven as suitable attaching subunits for the fullerene derivatives upgrading,<sup>21</sup> two diglycino-derivatives containing different symmetric polyoxa-spacers were chosen as substrates and subjected to biscycloaddition to C<sub>60</sub> in the presence of formaldehyde. Here we present the results of one-pot double Prato reaction, together with electrochemical, self-ordering, and *in vitro* antioxidant properties of obtained products.

## 2 Results and discussion

### 2.1 Synthesis

In intention to examine the selectivity of one-pot biscycloaddition of polyoxa-bridged diglycines to C<sub>60</sub>, starting diamines **1** and **2** were subjected to the synthetic sequence presented in Scheme 1. A simultaneous double mono-alkylation by benzyl-bromoacetate (BBA) afforded corresponding dibenzyl esters **3** and **4** in satisfactory yields, and further Pd-C catalysed hydrogenolysis led to diglycines **5** and **6** almost quantitatively. Following the procedure previously optimised for similar alkyl-analogues,<sup>20</sup> a suspension of obtained products and 10-fold molar excess of formaldehyde in ODCB at elevated temperature (160 °C) was *in situ* transformed to corresponding azomethineylides which underwent double [3 + 2]-cycloaddition to an equimolar amount of C<sub>60</sub>.

The *cis*-2 isomer was obtained as a major product in both reactions, but better selectivity was achieved by employing the shorter chain (Fig. 1). Thus, diglycine **5**, containing dioxo-spacer gave exclusively bridged bispyrrolidinofullerenes in overall yield of 27%. Only three of eight possible isomeric bisadducts were isolated, *cis*-1 (**7**), *cis*-2 (**8**) and *cis*-3 (**9**) in 1 : 7.4 : 2.6 ratio, respectively. Under the same conditions diglycine **6** with three ether subunits in bridging chain reacted somewhat less selectively affording the mixture of four bispyrrolidino adducts **10**–**13** (24%) together with dumbbell-like difullerene derivative **14** (3%). As in previous case, the *cis*-2 compound was isolated as a major product, but with lower prevalence, so the product ratio followed the order *cis*-1 (**10**) : *cis*-2 (**11**) : *cis*-3 (**12**) : *eq* (**13**) = 1 : 4.8 : 2.8 : 1.3. It should be noted that the formation of the dumbbell-bisfulleropyrrolidine was achieved without a large excess of the C<sub>60</sub>, which was usually applied for the synthesis of such compounds.<sup>22</sup>

Both reaction mixtures were separated easily, by SiO<sub>2</sub> dry column flash chromatography using toluene to collect unreacted C<sub>60</sub> and toluene/EtOAc mixtures for individual compounds.

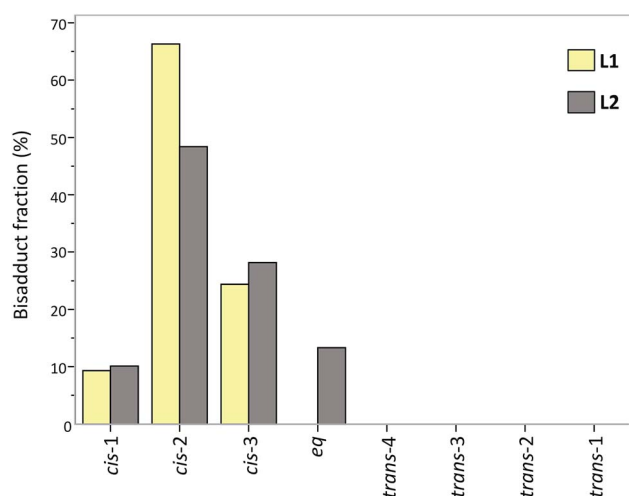
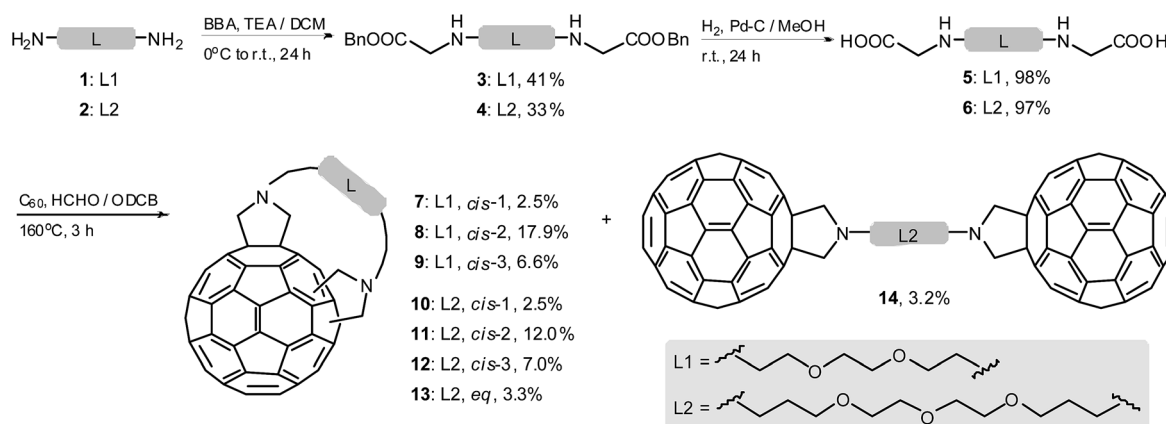


Fig. 1 Relative distribution of isolated bisadducts bridged with 3,6-dioxaoctyl (L1) and 4,7,10-trioxatridecyl linker (L2).



Scheme 1 Synthesis of fullerene derivatives containing 3,6-dioxaoctyl (L1) and 4,7,10-trioxatridecyl linkers (L2).

The purity of all the compounds was checked by the HTPLC. Functionalization of the fullerene sphere led to the significant improvement of compounds solubility in chloroform, ranging from 10 mg mL<sup>-1</sup> for dumbbell-compound **14**, to 20 and 40 mg mL<sup>-1</sup> for bisadducts bridged by dioxa and trioxa-chain, respectively. In such a way their full spectral characterization and investigation of morphological, electrochemical and anti-oxidant features was significantly facilitated.

## 2.2 Structure determination

The structures of compounds **7–14** were fully confirmed by IR, UV/Vis, 1D (<sup>1</sup>H/<sup>13</sup>C) and 2D (COSY and HSQC) NMR spectroscopy and by HR (ESI-TOF) mass spectrometry. Among the spectroscopic methods employed, a comparative analysis of UV-vis and NMR spectra gave the crucial proof on their addition patterns. The spectra of isolated compounds presenting absorption behaviour in visible region are superimposed in Fig. 2. Difullerene adduct **14** showed a sharp peak at 431 nm and a broader one at 698 nm, which are characteristic absorptions of fulleropyrrolidine monoadducts.<sup>23</sup> Both set of the *cis*-bisadducts containing shorter L1 and longer L2 linker (**7–9** and **10–12**, respectively) showed almost identical absorption properties with notable variations among compounds within each series (Fig. 2). In addition, observed distinct absorption patterns in the 400–750 nm visible region were similar to those reported for bis(pyrrolidino)fullerenes bridged by alkyl-tether,<sup>20</sup> as well as to other C<sub>60</sub> bisadducts,<sup>24</sup> such confirming the major impact of the fullerene chromophore and addition pattern on the absorption properties.

The addition patterns of bisadduct regioisomers have also been corroborated by the molecular symmetry deduced from their <sup>1</sup>H and <sup>13</sup>C NMR spectra (*C<sub>s</sub>* symmetry for *cis*-1, *cis*-2, and *eq*; *C<sub>2</sub>* symmetry for *cis*-3).<sup>11d,20</sup> The expanded <sup>1</sup>H and <sup>13</sup>C NMR spectral regions of all the products **7–14** are presented in Fig. 3 and 4, respectively. Each of the bisadducts gave unique pattern for the fullerene C-atoms, as well as the pyrrolidine and tether carbons and protons. With the exception of the equatorial isomer **13**, all other bisadducts **7–12** gave the two pairs of doublets ( $\delta = 3.3\text{--}5.3$  ppm) belonging to the two pyrrolidinic rings with geminal coupling constants of about 10 Hz and significant chemical shift difference. Furthermore, two well defined multiplets (dd, ddd or dt) corresponding to the geminal protons of the two terminal methylene CH<sub>2</sub> groups (H<sup>1,8</sup> and H<sup>1',8'</sup> for **7–9** or H<sup>1,13</sup> and H<sup>1',13'</sup> for **10–12**) are observed in the range of  $\delta$  2.8–3.7 ppm, indicating their equivalence. Additionally, the distinctive multiplet signals of the ether methylene protons (CH<sub>2</sub> (2,7; 4,5) for **7–9** and CH<sub>2</sub> (3,11; 5,9; 6,8) for **10–12**), largely overlapped in a narrow range of  $\delta$  3.7–4.0 ppm, while the methylene CH<sub>2</sub>(2,12) protons of the *cis* regioisomers **10–12** appeared as a symmetric multiplet signal at a higher field ( $\delta$  2.0–2.2 ppm). The <sup>1</sup>H NMR spectrum of the equatorial bisadduct **13** showed two singlets ( $\delta$  4.01 and 4.10 ppm) belonging to the pyrrolidinic ring positioned in the mirror plane, and two doublets ( $\delta$  4.42 and 3.80 ppm) of the perpendicularly oriented one. In addition, the 10 nonequivalent methylene groups of the tether, located in the mirror plane gave triplets at  $\delta$  3.10 and 3.08 ppm (CH<sub>2</sub>(1,13)), quintets at  $\delta$  1.98 and 2.04 ppm

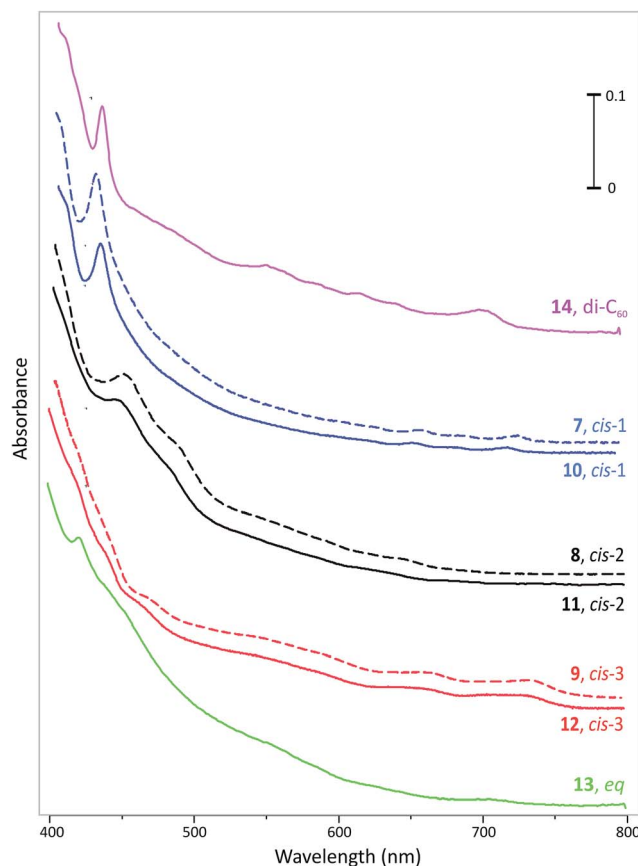


Fig. 2 The visible region of the UV-vis spectra of di-C<sub>60</sub> adduct **14** and the seven regioisomeric fulleropyrrolidine bisadducts (**7–13**) in toluene.

(CH<sub>2</sub>(2,12)), and the remaining multiplet signals in the range of  $\delta$  3.48–3.82 ppm for the ether CH<sub>2</sub>-groups (Fig. 3).

The expanded sp<sup>2</sup> and sp<sup>3</sup> C regions of the <sup>13</sup>C NMR spectra of compounds **7–14** with a clear difference in the number, distribution and intensities of the fullerene signals between regioisomers are presented in Fig. 4. The chemical shifts of the fullerene subunits in the *cis*-bisadducts **7–12** were shown to be independent of the bridge structure, and almost identical values were observed for each individual isomer containing both shorter L1 and longer L2 moiety (Table S2,† the *cis*-1, *cis*-2 and *cis*-3 couples **7/10**, **8/11** and **9/12**, respectively). The presence of half signals belonging to the 56 fullerene, 4 pyrrolidine, and 6 or 10 tether carbons in all the *cis* regioisomers indicated the presence of the mirror plane bisecting the fullerene cage, as well as the tether. All observed motifs were in agreement with the corresponding molecular symmetry.<sup>11d,20</sup> Thus, in the area of  $\delta = 130\text{--}160$  ppm, corresponding to the fullerene sp<sup>2</sup> C responses, *C<sub>s</sub>* symmetric *cis*-1 and *cis*-2 compounds gave 30 peaks (26 + 4 with the intensities 2C and 1C, respectively), while *C<sub>2</sub>* symmetric *cis*-3 bisadducts showed 28 signals (with intensity 2C). The region of  $\delta$  65–72 ppm contained two pairs of peaks, belonging to the quaternary and the secondary pyrrolidine carbons, together with 2 or 3 signals of C–O nuclei from the tether. The terminal bridge carbons gave 1 signal at  $\delta = 50\text{--}53$  ppm, and both remaining C(2,12) from the longer L2 bridge resonated at  $\delta = 29$  ppm. The

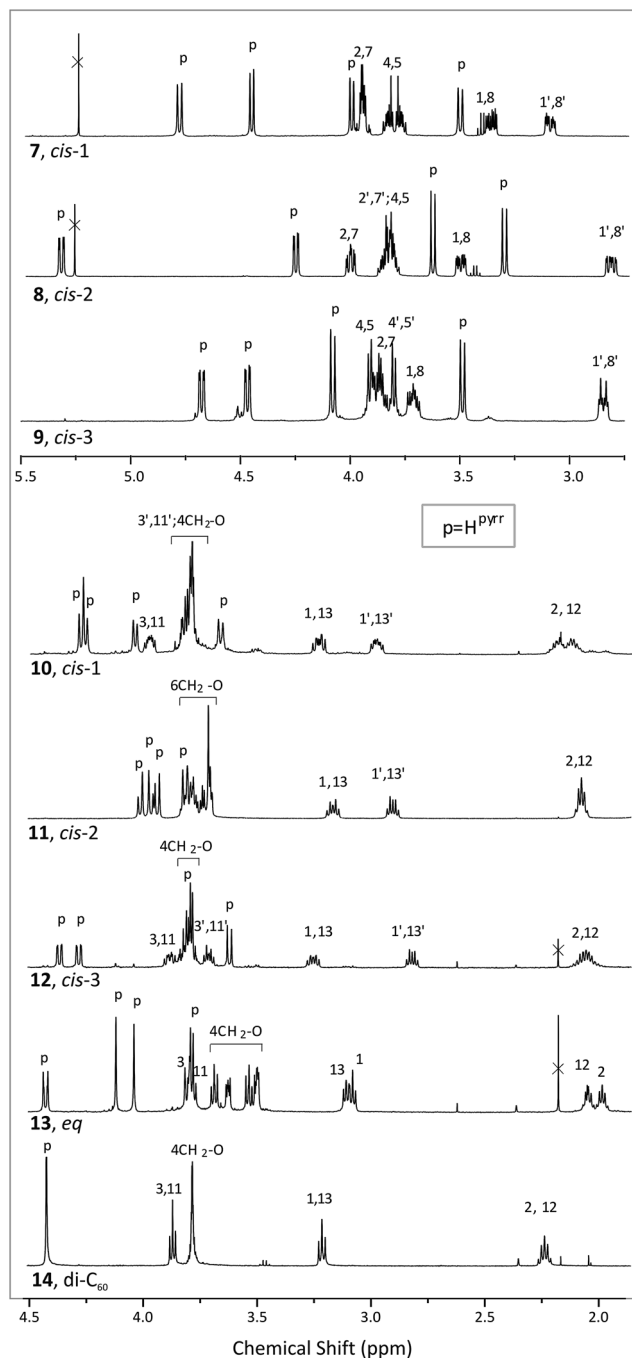


Fig. 3  $^1\text{H}$  NMR spectra of the regioisomeric bisadducts containing the 3,6-dioxaoctane chain (7–9), 4,7,10-trioxatridecane chain (10–13), and di- $\text{C}_{60}$  adduct 14.

equatorial bisadduct 13 showed different  $^{13}\text{C}$  NMR pattern with 29 fullerene  $\text{sp}^2$  C responses (27 with the intensity of 2C and 2 with the intensity of 1C), two set of three signals belonging to the fullerene  $\text{sp}^3$  and pyrrolidine carbons (both containing 2 + 1 signals with intensities 1C and 2C, respectively), as well as ten peaks originating from the mirror plane located trioxatridecane chain (Fig. 4).

The NMR spectra of difullerene 14 completely reflected its  $\text{C}_{2v}$  symmetry. Chemically and magnetically equivalent protons

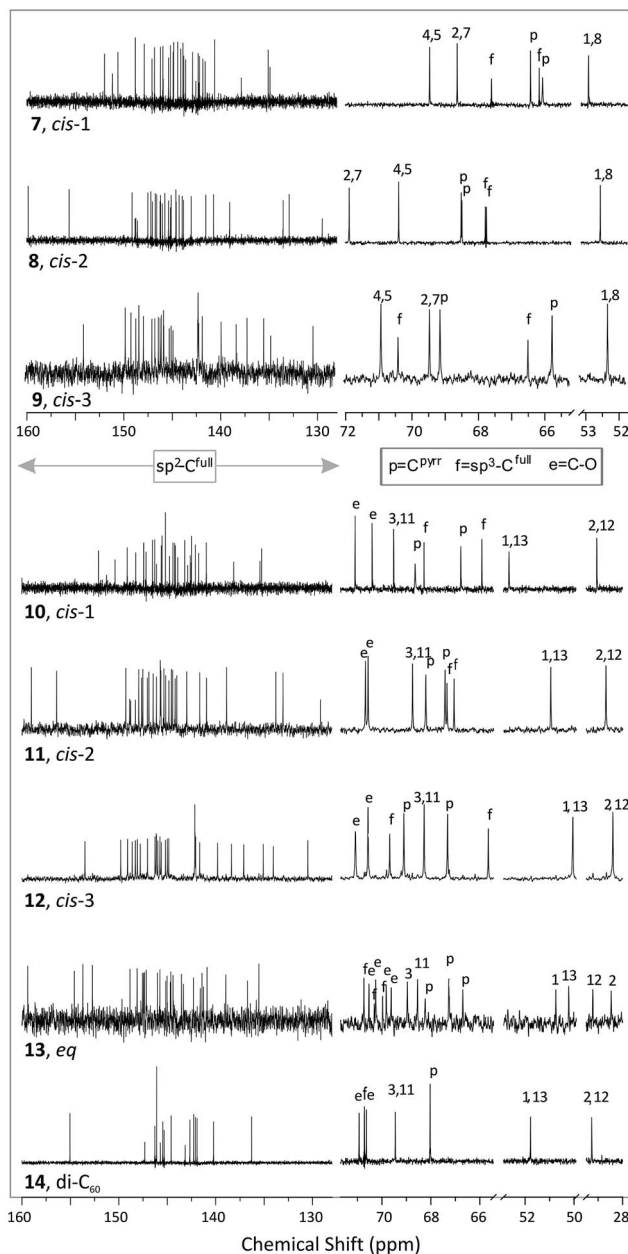


Fig. 4 Comparison of the fullerenic and aliphatic  $^{13}\text{C}$  NMR spectral regions of the fulleropyrrolidine bisadducts containing the 3,6-dioxaoctane chain (7–9), 4,7,10-trioxatridecane chain (10–13), and di- $\text{C}_{60}$  adduct 14.

of the pyrrolidine rings appeared as one singlet at  $\delta$  4.42 ppm. The propylene subunits of the tether gave two triplets at  $\delta$  = 3.86 and 3.21 ppm ( $\text{CH}_2$   $^{3,11}$  and  $\text{CH}_2$ ,  $^{1,13}$  respectively) and the quintet at  $\delta$  = 2.23 ppm ( $\text{CH}_2$   $^{2,12}$ ), while the resonances of the remaining internal ethylene moieties superimposed into a fine singlet at  $\delta$  3.78 ppm (Fig. 3). The  $^{13}\text{C}$  NMR spectrum contained a group of 15  $\text{sp}^2$  fullerene signals at  $\delta$  = 155–136 ppm, distributed in a pattern of 1 + 11 + 3 peaks with intensities 16, 8 and 4C, respectively. Five signals, corresponding to the fullerene  $\text{sp}^3$  C, pyrrolidine carbons and three groups of C–O units appeared in the region of  $\delta$  = 68–71 ppm, while the two terminal bridge constituents  $\text{C}^{1,13}$  and  $\text{C}^{2,12}$  resonated at a higher

field (52 and 29 ppm, respectively). In addition a molecular ion of compound **14**, observed at  $m/z$  1713, confirmed the presence of two fullerene subunits.

### 2.3 Morphology

The ability of the  $C_{60}$  and its derivatives to assemble into ordered supramolecular architectures with controllable size, morphology and structure was extensively studied.<sup>25</sup> The fullerene cage along with the attached moieties governed the self-assembly, leading to the formation of different one- to three-dimensional supramolecular nanostructures.<sup>26,10b</sup> Furthermore, a notable effect of the external stimuli (solvent polarity, temperature, pH, light, ultrasound) on the final morphology has also been observed.<sup>27</sup> In our previous work it has been shown that both addition pattern and the connecting moiety expressed a remarkable influence on the self-assembly of alkyl tethered bis(pyrrolidino)fullerenes.<sup>20</sup> Therefore, we assume that new fullerene containing bisadducts **7–13**, together with dumbbell-like difullerene compound **14** offer the possibility to study the synergistic effects of the polar oxalkane chain and the fullerene cage on the self-assembly process.

The morphology and size of supramolecular assemblies of compounds **7–14** were studied by means of SEM using dried samples obtained by a slow evaporation of dilute solution<sup>28</sup> in individual solvents and solvent binary systems of different polarity (PhMe, ODCB,  $CHCl_3$ , PhMe/*i*-PrOH (1 : 1) and PhMe/dioxane (1 : 1)) on a glass substrate at room temperature. Selected results are presented in Fig. 5, while additional pictures of all performed experiments are collected in ESI.†

The detailed analysis of the SEM images revealed no strong influence of the solvent on the primarily formed nanoparticles. In all tested environments the obtained self-assemblies were made up of quite similar, circular to oval particles (Fig. 5a and b and ESI†), indicating the prevalence of intermolecular interactions over the solvent-solute ones. The *cis*-bisadducts **7–9** further organized to compact, densely packed multilayered spherical structures (Fig. 5c) or flower-arranged petals (Fig. 5d and S52†) with dimensions in the range of 5–20  $\mu m$ . On the other hand, the initial oval particles of compounds bridged by longer tether (**10–14**) formed diverse

aggregates, such as circularly arranged microflakes of the *cis*-2 **11** (Fig. 5e), film-like irregular networks of the *cis*-3 **12** (Fig. 5f) and the *cis*-1 **10** (Fig. S53†), and the highly unordered microstructure of the *equatorial* isomer **13** (Fig. S53†). The SEM images of dumbbell-like fullerene derivative **14** with two bulky  $C_{60}$  at both ends of the chain (Fig. 5g), revealed quite different flower shaped morphology composed of the rectangular multilayered plates, once again indicating the overriding influence of the structure on the self organization in comparison to the environmental conditions. The only exception was the *cis*-2 compound **8** where the solvent-induced polymorphism, extensively studied by Nakanishi and coworkers,<sup>29</sup> was observed. Thus, a low level of self-ordering was achieved in all individual solvents, while in their more polar mixtures very large well-organized star-like forms (built of spindle rod particles) were formed (Fig. S52†).

### 2.4 Electrochemical properties

The electrochemical properties of the bisadducts **7–13** and difullerene **14** were investigated by cyclic voltammetry in 1 mM solutions at room temperature. Voltammograms were recorded in two different solvents, ODCB/DMF 2 : 1 and DCM, both accompanied with TBAP as a supporting electrolyte and calibrated with ferrocene/ferrocenyl couple ( $Fc/Fc^+$ ) as an internal standard. In addition, an influence of the bridge structure and length on the electrochemical behaviour was examined along the series of compounds with equally positioned, but variously tethered pyrrolidine rings. To that purpose, the electrochemical data of the *cis*-2 adducts **8** and **9**, achieved in ODCB/DCM 2 : 1 mixture at the scan rate  $0.7 V s^{-1}$  and in the presence of TBAP, were compared to those collected for already known alkyl tethered *cis*-2 adducts **15–19**<sup>20</sup> under the same conditions. Detected distortion of the cyclic voltammograms, with anodic to cathodic half-waves separation higher than 60 mV could be attributed to an attenuated electron transfer and the uncompensated resistance, as it was previously observed both for the reference  $Fc/Fc^+$  system<sup>30</sup> and fullerene derivatives.<sup>31</sup>

In the solvent mixture all fulleropyrrolidines showed three successive, reversible, fullerene-centred one-electron reductions, while mainly two of them, both located at more positive values were detected in DCM (Table 1). The presence of ODCB in the solvent mixture significantly lowered a total electron-accepting ability of the medium (defined by  $E_T^N$ ) resulting in reduced stabilization of formed anions and hindered reduction.<sup>32</sup> Nevertheless, the appearance of only two, quite broad redox waves, as well as an insufficient solubility of alkyl tethered bisadducts **15–19** in DCM, prompted us to continue investigation using ODCB/DMF mixture. As expected, the fullerene functionalization and consequent double bond saturation aggravated reduction, so the half-wave potentials corresponding to the first reduction were up to 300 mV negatively shifted in comparison to the pristine  $C_{60}$ . However, no regular change of the reduction potential with increasing the number of addends was observed, indicating a long-range electron-withdrawing effect of the second fullerene moiety in the dumbbell mono-adduct **14**.

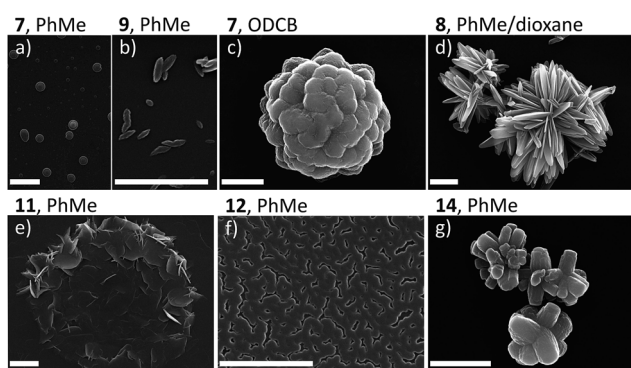
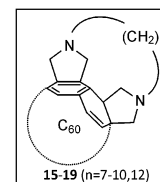


Fig. 5 The SEM images of self-organized assemblies of selected bisadducts prepared by a solvent evaporation of a dilute solution on a glass substrate at room temperature. Scale bars correspond to 5  $\mu m$ .

**Table 1** The half-wave potentials ( $E_{1/2}$ ) of the first (I), second (II) and third reduction (III) and energy gaps ( $\Delta E$ ) of compounds 7–19 recorded in ODCB/DMF 2 : 1 and DCM with TBAP as supporting electrolyte, at scanning rate of  $0.7 \text{ V s}^{-1}$

Compound		$E_{1/2}$ (V vs. Fc/Fc <sup>+</sup> ) ODCB/DMF 2 : 1					$E_{1/2}$ (V vs. Fc/Fc <sup>+</sup> ) DCM		
		I	II	III	$\Delta E^{\text{I-II}}$	$\Delta E^{\text{II-III}}$	I	II	III
<i>cis</i> -1	7	-1.51	-1.95	-2.65	0.44	0.70	-1.33	-1.72	
	10	-1.46	-1.96	-2.73	0.50	0.77	-1.29	-1.70	-2.34
<i>cis</i> -2	8	-1.36	-1.79	-2.47	0.43	0.68	-1.37	-1.75	
	11	-1.33	-1.77	-2.42	0.44	0.65	-1.35	-1.74	
	15	-1.37	-1.79	-2.40	0.42	0.71			
	16	-1.34	-1.78	-2.48	0.44	0.70			
	17	-1.32	-1.77	-2.48	0.45	0.71			
	18	-1.33	-1.77	-2.46	0.44	0.69			
	19	-1.34	-1.78	-2.44	0.44	0.66			
<i>cis</i> -3	9	-1.59	-2.04	-2.57	0.45	0.53	-1.40	-1.82	-2.31
	12	-1.57	-2.03	-2.58	0.46	0.55	-1.39	-1.81	-2.31
<i>Eq</i>	13	-1.55	-1.98	-2.66	0.44	0.68	-1.35	-1.76	
Di	14	-1.41	-1.87	-2.49	0.46	0.62			
	C <sub>60</sub>	-1.28	-1.74	-2.27	0.46	0.53			



Thus, the lowest shift was observed for the *cis*-2 compounds (40–90 mV), somewhat higher for compound 14 (130 mV) and the highest value of 200–300 mV for the rest of compounds containing the *cis*-1, *cis*-3 and *equatorially* positioned pyrroline rings (Fig. 6). As can be seen from Table 1, no significant influence of the tether length nor the structure on the electrochemical behaviour of tested compounds was found. The reduction potentials corresponding to individual regioisomers appeared at the similar values, regardless the presence of L1, L2 or C7–C12 linker (Table 1, compounds 7 and 10 (*cis*-1); 8, 11 and 15–19 (*cis*-2); or 9 and 12 (*cis*-3)). On the other hand, a variation of the addition pattern provoked different distortion of the  $\pi$ -electronic system of the carbon sphere, resulting in a quite different schedule of the corresponding potential maxima.<sup>33</sup> Values of the first potential gap ( $\Delta E_{1/2}^{\text{I-II}}$ ) in ODCB/DMF mixture of all compounds were distributed in a range from 0.43 to 0.50 V (mostly in a narrow radius of 0.44–0.45 V), while in DCM the CV curves of the *cis*-2 compounds 8 and 11 were constricted in comparison to other bisadducts ( $\Delta E_{1/2}^{\text{I-II}} \sim 0.30$  and 0.40 V, respectively). In contrast, the magnitude of the second potential gap ( $\Delta E_{1/2}^{\text{II-III}}$ ) varied considerably with the addition pattern on the carbon core. The values from  $\sim 0.53$  V for the *cis*-3 compounds, over 0.6–0.7 V for monoadduct 14, the *cis*-2 and the *equatorial* isomers to almost 0.8 V for the *cis*-1 compounds were detected on the CV curves obtained from ODCB/DCM solution, whereas no enough data were achieved from experiment performed in DCM.

## 2.5 Antioxidant capacity

The ability of the fullerene core to express the antioxidant activity is usually minimized by its poor solubility in both polar and nonpolar media. As it mentioned before, the introduction of the polyoxa-moiety provided compounds with slightly reduced electron-accepting affinity. At the same time, the presence of the tether significantly improved the solubility in

organic solvents and facilitated liposome formation, such giving a possibility to investigate the radical scavenging capacity in water environment. Loading soybean lecithin with

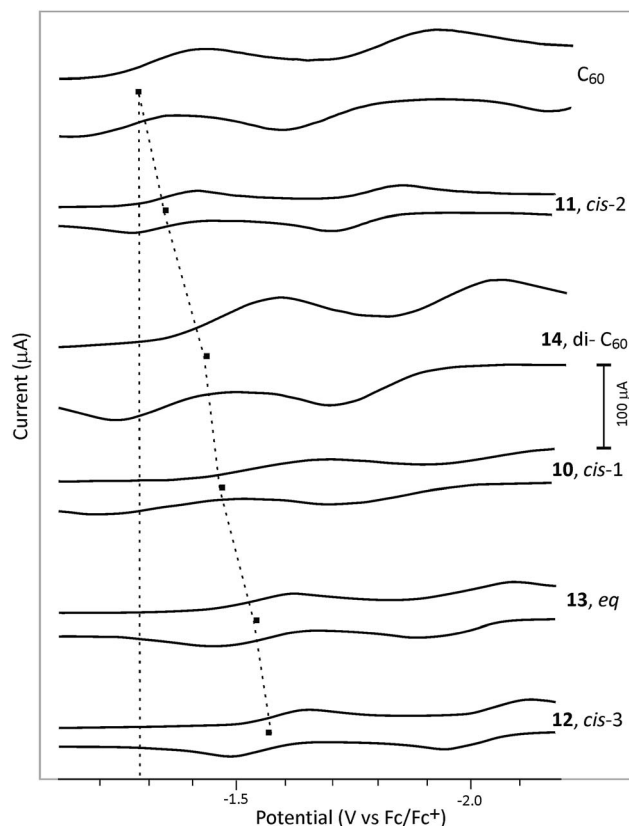


**Fig. 6** Shifts in half-wave potentials of the first reduction with the change of the addition pattern on the carbon core. Figure presents parts of the cyclic voltammograms of adducts 10–14 and of parent C<sub>60</sub>, recorded in ODCB/DMF 2 : 1 with TBAP as supporting electrolyte, at scanning rate  $0.7 \text{ V s}^{-1}$ .

**Table 2** Antioxidant activities *in vitro* of liposomal form of compounds 7–14 against H<sub>2</sub>O<sub>2</sub> and TBHP, expressed as a direct percentage of quenched peroxide ( $\Delta$ ), and relative activities recalculated to the molar ratio 1 : 1 (AOA<sub>molar</sub>), toward vitamin C and parent C<sub>60</sub>

Compound	$\Delta$ (%)		AOA <sub>molar</sub> vs. vit C		AOA <sub>molar</sub> vs. C <sub>60</sub>	
	H <sub>2</sub> O <sub>2</sub>	TBHP	H <sub>2</sub> O <sub>2</sub>	TBHP	H <sub>2</sub> O <sub>2</sub>	TBHP
7, <i>cis</i> -1	–23.7	–23.0	9.1	10.3	1.6	1.8
8, <i>cis</i> -2	–23.4	–22.3	8.9	10.0	1.6	1.7
9, <i>cis</i> -3	–23.8	–23.1	9.1	10.3	1.6	1.8
10, <i>cis</i> -1	–23.2	–24.1	9.5	11.6	1.7	2.0
11, <i>cis</i> -2	–22.1	–22.0	9.1	10.6	1.6	1.8
12, <i>cis</i> -3	–22.7	–22.2	9.4	10.7	1.6	1.8
13, <i>eq</i>	–22.1	–22.8	9.1	11.0	1.6	1.9
14, di-C <sub>60</sub>	–24.8	–23.9	17.6	19.8	3.1	3.4
C <sub>60</sub>	–19.0	–16.7	5.7	5.8	1.0	1.0
Vitamin C	–13.7	–11.7	1.0	1.0	0.2	0.2

compounds 7–14 and the fullerene C<sub>60</sub> provided fullerosomes which were subjected to the FOX protocol<sup>34</sup> in the presence of *tert*-butylhydroperoxide (TBHP) or H<sub>2</sub>O<sub>2</sub> as sources of peroxides, and vitamin C as a positive control. Obtained results are collected in Table 2, and more detailed explanation is given in ESI.† Quite uniform activities toward both peroxides, approximately 10-fold higher than vitamin C and 1.5 to 2 times higher than parent C<sub>60</sub> were observed along whole series of bisadducts 7–13. Although differed in the electrochemical and morphological properties, all synthesized compounds showed nearly equal antioxidant capacity, indicating no strong influence of such parameters on radical quenching process. It might be supposed that suppressed aggregation, resulted from the solubility improvement after functionalization, reinforced an expression of the antioxidant potential of the fullerene core. As expected, the activity of compound 14 with two fullerene subunits was almost duplicated relative to other derivatives (Table 2). It is important to note that regardless of the double functionalization, performed derivatization led to the improvement of the radical scavenging capacity, since all of the synthesized compounds have proven to be more active than the parent C<sub>60</sub>.

### 3 Conclusions

In conclusions, the dioxaalkyl-tethered diglycine has proven to be a suitable template for the preparation of *cis*-bispyrrolidino-fullerenes. The prolongation of the tether led to the mixture of four bisadducts (all *cis* and the *equatorial* one) and difullerene dumbbell monoadduct, although reaction conditions were adjusted to the bisadducts synthesis. The structure of each compound was unambiguously determined by comparative analysis of the spectral data, considering also the molecular symmetry. Much better solubility in comparison to pristine C<sub>60</sub> facilitated property investigations. All compounds underwent highly ordered self-assembling giving hierarchically organized aggregates, the ultimate form of which depended on the chain structure and a spatial orientation of the pyrrolidine rings, as well. No solvent induced polymorphism was observed, except for

the *cis*-2 bispyrrolidino fullerene bearing dioxa tether. Furthermore, the electrochemical properties of obtained compounds depended on the electroactive (fullerene) subunit and its addition pattern. Finally, despite hindered electron-accepting ability all compounds expressed a significant *in vitro* radical scavenging capacity, which turned out to be independent on the addition pattern as well as the investigated properties, and could be the consequence of improved solubility. The compound containing two fullerene subunits reached the highest activity, appearing more potent than vitamin C, C<sub>60</sub> and all the bisadducts for the order of magnitude 20, 5 and 2, respectively.

### Acknowledgements

This research has been supported by Serbian Ministry of Education, Science and Technological development, grant 172002.

### Notes and references

- (a) M. Prato, *J. Mater. Chem.*, 1997, 7, 1097; (b) Y.-Y. Lai, Y.-J. Cheng and C.-S. Hsu, *Energy Environ. Sci.*, 2014, 7, 1866; (c) F. Wudl, *J. Mater. Chem.*, 2002, 12, 1959; (d) C. Wang, Z.-X. Guo, S. Fu, W. Wu and D. Zhu, *Prog. Polym. Sci.*, 2004, 29, 1079; (e) B. I. Kharisov, O. V. Kharissova, M. J. Gomez and U. O. Mendez, *Ind. Eng. Chem. Res.*, 2009, 48, 545.
- (a) R. Bakry, R. M. Vallant, M. Najam-ul-Haq, M. Rainer, Z. Szabo, C. W. Huck and G. K. Bonn, *Int. J. Nanomed.*, 2007, 2, 639; (b) X. Yang, A. Ebrahimi, J. Li and Q. Cui, *Int. J. Nanomed.*, 2014, 9, 77.
- (a) C. Bingel, *Chem. Ber.*, 1993, 126, 1957; (b) D. He, X. Du, Z. Xiao and L. Ding, *Org. Lett.*, 2014, 16, 612; (c) M. Carano, C. Corvaja, L. Garlaschelli, M. Maggini, M. Marcaccio, F. Paolucci, D. Pasini, P. P. Righetti, E. Sartori and A. Toffoletti, *Eur. J. Org. Chem.*, 2003, 374; (d) D. Felder, D. Guillon, R. Lévy, A. Mathis, J.-F. Nicoud, J.-F. Nierengarten, J.-L. Rehspringer and J. Schell, *J. Mater. Chem.*, 2000, 10, 887.
- (a) J. B. Briggs and G. P. Miller, *C. R. Chim.*, 2006, 9, 916; (b) G. H. Sarova and M. N. Berberan-Santos, *Chem. Phys. Lett.*, 2004, 397, 402; (c) L. M. Giovane, J. W. Barcot, T. Yadav, A. L. Lafleur, J. A. Marr, J. B. Howard and V. M. Rotello, *J. Phys. Chem.*, 1993, 97, 8560.
- (a) M. Maggini, G. Scorrano and M. Prato, *J. Am. Chem. Soc.*, 1993, 115, 9798; (b) M. Prato and M. Maggini, *Acc. Chem. Res.*, 1998, 31, 519; (c) K. Kordatos, T. Da Ros, S. Bosi, E. Vázquez, M. Bergamin, C. Cusan, F. Pellarini, V. Tomberli, B. Baiti, D. Pantarotto, V. Georgakilas, G. Spalluto and M. Prato, *J. Org. Chem.*, 2001, 66, 4915; (d) S. Aroua, W. B. Schweizer and Y. Yamakoshi, *Org. Lett.*, 2014, 16, 1688.
- (a) Y. He and Y. Li, *Phys. Chem. Chem. Phys.*, 2011, 13, 1970; (b) E. Voroshazi, K. Vasseur, T. Aernouts, P. Heremans, A. Baumann, C. Deibel, X. Xue, A. J. Herring, A. J. Athans, T. A. Lada, H. Richtere and B. P. Rand, *J. Mater. Chem.*, 2011, 21, 17345; (c) Y. He, H.-Y. Chen, J. Hou and Y. Li, *J. Am. Chem. Soc.*, 2010, 132, 1377; (d) S. Campidelli,

- E. Vázquez, D. Milic, J. Lenoble, C. A. Castellanos, G. Sarova, D. M. Guldi, R. Deschenaux and M. Prato, *J. Org. Chem.*, 2006, **71**, 7603; (e) S. Bosi, T. Da Ros, G. Spalluto, J. Balzarini and M. Prato, *Bioorg. Med. Chem. Lett.*, 2003, **13**, 4437.
- 7 A. Hirsch, *Top. Curr. Chem.*, 1999, **199**, 1–65.
- 8 (a) N. F. Gol'dshleger, A. N. Lapshin, E. I. Yudanov, N. M. Alpatova and E. V. Ovsyannikova, *Russ. J. Electrochem.*, 2006, **42**, 16; (b) T. Suzuki, Y. Maruyama, T. Akasaka, W. Ando, K. Kobayashi and S. Nagasaka, *J. Am. Chem. Soc.*, 1994, **116**, 1359; (c) D. M. Guldi, H. Hungerbühler and K.-D. Asmus, *J. Phys. Chem.*, 1995, **99**, 9380.
- 9 B. M. Illescas and N. Martín, *C. R. Chim.*, 2006, **9**, 1038.
- 10 (a) P. Zhang, Z. X. Guo and S. Lv, *Chin. Chem. Lett.*, 2008, **19**, 1039; (b) S. Zhou, J. Ouyang, P. Golas, F. Wang and Y. Pan, *J. Phys. Chem. B*, 2005, **109**, 19741.
- 11 (a) A. Hirsch, I. Lamparath and H. R. Karfunkel, *Angew. Chem., Int. Ed. Engl.*, 1994, **33**, 437; (b) M. W. J. Beulen, J. A. Rivera, M. Á. Herranz, B. Illescas, N. Martín and L. Echegoyen, *J. Org. Chem.*, 2001, **66**, 4393; (c) Q. Lu, D. I. Schuster and S. R. Wilson, *J. Org. Chem.*, 1996, **61**, 4764; (d) K. Kordatos, S. Bosi, T. Da Ros, A. Zamboni, V. Lucchini and M. Prato, *J. Org. Chem.*, 2001, **66**, 2802; (e) A. Duarte-Ruiz, T. Müller, K. Wurst and B. Kräutler, *Tetrahedron*, 2001, **57**, 3709.
- 12 R. Wilson and Q. Lu, *Tetrahedron Lett.*, 1995, **36**, 5707.
- 13 (a) L. Isaacs, R. F. Haldimann and F. Diederich, *Angew. Chem., Int. Ed.*, 1994, **33**, 2339; (b) L. Isaacs, F. Diederich and R. F. Haldimann, *Helv. Chim. Acta*, 1997, **80**, 317.
- 14 J.-F. Nierengarten, V. Gramlich, F. Cardullo and F. Diederich, *Angew. Chem., Int. Ed. Engl.*, 1996, **35**, 2101.
- 15 Y. Ishida, H. Ito, D. Mori and K. Saigo, *Tetrahedron Lett.*, 2005, **46**, 109.
- 16 (a) J.-P. Bourgeois, F. Diederich, L. Echegoyen and J.-F. Nierengarten, *Helv. Chim. Acta*, 1998, **81**, 1835; (b) L. R. Sutton, M. Scheloske, K. S. Pirner, A. Hirsch, D. M. Guldi and J.-P. Gisseelbrecht, *J. Am. Chem. Soc.*, 2004, **126**, 10370; (c) J. Ranta, T. Kumpulainen, H. Lemmetyinen and A. Efimov, *J. Org. Chem.*, 2010, **75**, 5178.
- 17 J.-P. Bourgeois, L. Echegoyen, M. Fibbioli, E. Pretsch and F. Diederich, *Angew. Chem., Int. Ed.*, 1998, **37**, 2118.
- 18 Z. Zhou, D. I. Schuster and S. R. Wilson, *J. Org. Chem.*, 2006, **71**, 1545.
- 19 G. Rotas and N. Tagmatarchis, *Tetrahedron Lett.*, 2009, **50**, 398.
- 20 T. Kop, M. Bjelaković and D. Milić, *Tetrahedron*, 2015, **71**, 4801.
- 21 (a) A. Mateo-Alonso, C. Soombar and M. Prato, *Org. Biomol. Chem.*, 2006, **4**, 1629; (b) S. Bosi, L. Feruglio, D. Milic and M. Prato, *Eur. J. Org. Chem.*, 2003, 4741; (c) K. Yoshimura, K. Matsumoto, Y. Uetani, S. Sakumichi, S. Hayase, M. Kawatsura and T. Itoh, *Tetrahedron*, 2012, **68**, 3605.
- 22 (a) R. Zalesny, O. Loboda, K. Iliopoulos, G. Chatzikyriakos, S. Couris, G. Rotas, N. Tagmatarchis, A. Avramopoulou and M. G. Papadopoulos, *Phys. Chem. Chem. Phys.*, 2010, **12**, 373; (b) J. K. Sørensen, J. Fock, A. Holmen Pedersen, A. B. Petersen, K. Jennum, K. Bechgaard, K. Kilså, V. Geskin, J. Cornil, T. Bjørnholm and M. Brøndsted Nielsen, *J. Org. Chem.*, 2011, **76**, 245; (c) D. Kreher, P. Hudhomme, A. Gorgues, H. Luo, Y. Araki and O. Ito, *Phys. Chem. Chem. Phys.*, 2003, **5**, 4583.
- 23 K. Kordatos, T. Da Ros, M. Prato, R. V. Bensasson and S. Leach, *Chem. Phys.*, 2003, **293**, 263.
- 24 (a) F. Djojo, A. Herzog, I. Lamparath, F. Hampel and A. Hirsch, *Chem.–Eur. J.*, 1996, **2**, 1537; (b) T. Ishi-I and S. Shinkai, *Tetrahedron*, 1999, **55**, 12515; (c) Y. Nakamura, N. Takano, T. Nishimura, E. Yashima, M. Sato, T. Kudo and J. Nishimura, *Org. Lett.*, 2001, **3**, 1193.
- 25 (a) D. M. Guldi, F. Zerbetto, V. Georgakilas and M. Prato, *Acc. Chem. Res.*, 2005, **38**, 38; (b) S. S. Babu, H. Möhwald and T. Nakanishi, *Chem. Soc. Rev.*, 2010, **39**, 4021; (c) L. K. Shrestha, R. G. Shrestha, J. P. Hill and K. Ariga, *J. Oleo Sci.*, 2013, **62**, 541.
- 26 (a) V. Georgakilas, F. Pellarini, M. Prato, D. M. Guldi, M. Melle-Franco and F. Zerbetto, *Proc. Natl. Acad. Sci. U. S. A.*, 2002, **99**, 5075; (b) K. H. L. Ho and S. Campidelli, *Adv. Nat. Sci.: Nanosci. Nanotechnol.*, 2014, **5**, 025008; (d) T. Nakanishi, Y. Shen, J. Wang, H. Li, P. Fernandes, K. Yoshida, S. Yagai, M. Takeuchi, K. Ariga, D. G. Kurth and H. Möhwald, *J. Mater. Chem.*, 2010, **20**, 1253.
- 27 (a) T. Nakanishi, *Chem. Commun.*, 2010, **46**, 3425; (b) H. Asanuma, H. Li, T. Nakanishi and H. Möhwald, *Chem.–Eur. J.*, 2010, **16**, 9330; (c) M. Yao, B. M. Andersson, P. Stenmark, B. Sundqvist, B. Liu and T. Wagberg, *Carbon*, 2009, **47**, 1181.
- 28 C. Park, H. J. Song and H. C. Choi, *Chem. Commun.*, 2009, 4803.
- 29 (a) T. Nakanishi, W. Schmitt, T. Michinobu, D. G. Kurthac and K. Ariga, *Chem. Commun.*, 2005, 5982; (b) T. Nakanishi, H. Takahashi, T. Michinobu, J. P. Hill, T. Teranishi and K. Ariga, *Thin Solid Films*, 2008, **516**, 2401.
- 30 N. G. Tsierkezos, *J. Solution Chem.*, 2007, **36**, 289.
- 31 B. Gigante, C. Santos, T. Fonseca, M. J. M. Curto, H. Luftmann, K. Bergander and M. N. Berberan-Santos, *Tetrahedron*, 1999, **55**, 6175.
- 32 D. Dubois, G. Moninot, W. Kutner, M. T. Jones and K. M. Kadish, *J. Phys. Chem.*, 1992, **96**, 7137.
- 33 M. Carano, T. Da Ros, M. Fanti, K. Kordatos, M. Marcaccio, F. Paolucci, M. Prato, S. Roffia and F. Zerbetto, *J. Am. Chem. Soc.*, 2003, **125**, 7139.
- 34 M. B. Lens, E. de Marni, R. Gullo, U. Citernes and R. Crippa, WO 043074 A1, 2007.